Transmission-Electron-Microscopy Studies of Small Dislocation Loops in $Al_{76}Si_4Mn_{20}$ Icosahedral Phase

Zhouguang Wang, Renhui Wang, and Wenfang Deng

Chinese Center of Advanced Science and Technology (World Laboratory), P.O. Box 8730, Beijing 100080, China and Department of Physics, Wuhan University, 430072 Wuhan, People's Republic of China

(Received 14 February 1991)

Small dislocation loops with characteristic diffraction contrast of black-white lobes have been observed experimentally in annealed $Al_{76}Si_4Mn_{20}$ quasicrystalline icosahedral phase by using transmission electron microscopy. The variation of the features of the diffraction-contrast images of the small dislocation loops with experimental conditions has been observed and computer simulated systematically. By taking the Burgers vector **b** and the normal **n** of the loops to be along the [100100] direction, i.e., parallel to one of the twofold symmetry axes, we have arrived at good agreement between the observed and computer-simulated features of the diffraction-contrast images.

PACS numbers: 61.70.Jc, 61.42.+h

In the studies of the radiation effect of crystals, the characteristics and their variation with the operating reflections and other experimental parameters of the electron-diffraction-contrast images of a small dislocation loop have been observed experimentally and calculated theoretically; see, e.g., Wilkens,[1] Saldin, Stathopoulos, and Whelan,[2] English, Eyre, Holmes, and Perrin,[3] and Edington.[4] It has been found that the contrast image of a small dislocation loop under the two-beam dynamical condition appears as a black-white lobe when it lies near the surfaces of the foil specimen and the angle between the Burgers vector **b** and the operating reflection **g** is not near the value of 90°.

Since the discovery of the quasicrystalline icosahedral phase (*i* phase) in rapidly quenched Al-Mn alloys,[5] many authors have studied defects in quasicrystals. In order to describe a defect in quasicrystals it is necessary to introduce the so-called phason strain in addition to the conventional phonon strain in crystals; see, e.g., Levine *et al.*[6] and Socolar, Lubensky, and Steinhardt.[7] Therefore, the Burgers vector **b** of a dislocation in icosahedral phase should be described by six indices and possess six components. Hirabayashi and Hiraga[8] observed dislocations in icosahedral Al-Mn phase and their phason strains by using high-resolution electron microscopy. Zhang, Wollgarten, and Urban[9] determined the Burgers vector **b** of dislocations in $Al_{65}Cu_{20}Fe_{15}$ icosahedral phase to be along the twofold axis by performing an electron-diffraction-contrast experiment. Dai and Wang[10] tried to obtain and simulate higher-order Laue zone (HOLZ) line patterns from quasicrystalline specimens and then Wang and Dai[11] observed the splitting and shifting of HOLZ lines caused by a line defect in $Al_{76}Si_4Mn_{20}$ icosahedral phase.

In the present paper we report our studies of small dislocation loops in $Al_{76}Si_4Mn_{20}$ icosahedral phase, including a systematic observation of the variation of their diffraction-contrast images with the operating reflection, and the corresponding computer simulation.

Rapidly solidified $Al_{76}Si_4Mn_{20}$ ribbons were annealed at 570 K for 3 h. The foils suitable for transmission electron microscopy (TEM) were prepared by argon-ion milling. TEM observations were performed by using a JEM-100CX(II) electron microscope equipped with a double-tilting stage ($\pm 45°$) operating at 120 kV.

The two-beam dynamical condition for the electron-diffraction-contrast observation has been obtained by using {211111}-type reflections which are parallel to the fivefold symmetry axes of the icosahedral phase. For $Al_{76}Si_4Mn_{20}$ *i* phase, the corresponding lattice plane distance $d_{211111}=0.217$ nm and the extinction distance $\xi_{g(211111)}$ was measured by Cheng and Wang[12] to be 94.2 nm by using a convergent-beam electron-diffraction

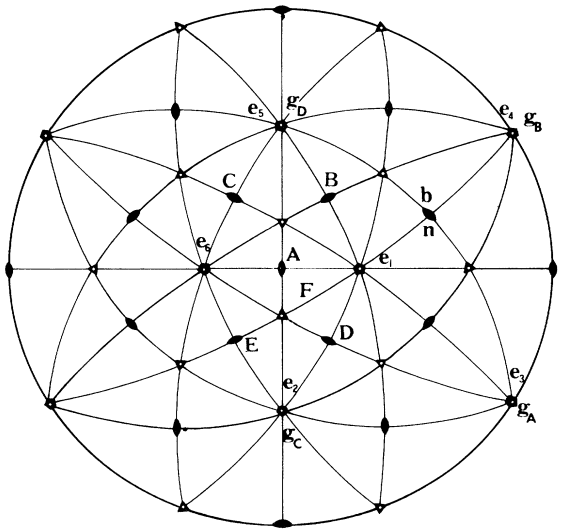

FIG. 1. Stereographic projection diagram of the *i* phase showing its basis vectors $\mathbf{e}_1$, $\mathbf{e}_2$, $\mathbf{e}_3$, $\mathbf{e}_4$, $\mathbf{e}_5$, and $\mathbf{e}_6$, twofold zone axes *A*, *B*, *C*, *D*, and *E*, and the directions of the {211111}-type reflections $\mathbf{g}_A$, $\mathbf{g}_B$, $\mathbf{g}_C$, and $\mathbf{g}_D$ along fivefold symmetry axes. The following symbols are used: **b**, Burgers vector; **n**, loop normal; **F**, foil normal; **B**, electron beam direction; *t*, foil thickness; *d*, depth of the center of the loop measured along the **F** direction; and *w*, deviation parameter.

TABLE I. Contrast features of the small dislocation loop under several beam directions and different reflections (where N denotes no contrast, BWL denotes black-white lobe, and IR denotes irregular contrast).

Beam direction	Reflection	Contrast feature
A [100001]	$\mathbf{g}_A$ $(11\bar{2}1\bar{1}\bar{1})$	N
	$\mathbf{g}_B$ $(1\bar{1}121\bar{1})$	BWL
B [100010]	$\mathbf{g}_C$ $(121\bar{1}\bar{1}1)$	N
	$\mathbf{g}_A$ $(11\bar{2}1\bar{1}\bar{1})$	N
C [000011]	$\mathbf{g}_B$ $(1\bar{1}121\bar{1})$	IR
	$\mathbf{g}_C$ $(121\bar{1}\bar{1}1)$	N
D [110000]	$\mathbf{g}_B$ $(1\bar{1}121\bar{1})$	BWL
	$\mathbf{g}_D$ $(1\bar{1}\bar{1}121)$	IR
E [010001]	$\mathbf{g}_D$ $(1\bar{1}\bar{1}121)$	IR
	$\mathbf{g}_A$ $(11\bar{2}1\bar{1}\bar{1})$	N

technique. By using a large-angle double-tilting stage it is usually possible to obtain five twofold zone axes labeled as A, B, C, D, and E in the stereographic projection diagram shown in Fig. 1. The $\{211111\}$-type reflections which appeared in these five-zone-axis patterns are $(11\bar{2}1\bar{1}\bar{1})$ $(\mathbf{g}_A)$, $(1\bar{1}121\bar{1})$ $(\mathbf{g}_B)$, $(121\bar{1}\bar{1}1)$ $(\mathbf{g}_C)$, and $(1\bar{1}\bar{1}121)$ $(\mathbf{g}_D)$, as shown in Fig. 1 and listed in Table I.

By using a conventional experimental method for obtaining a bright-field (BF) image and centered dark-field (DF) image,[4] one obtains a DF image under the operating reflection $-\mathbf{g}$ with a deviation parameter $-w$, when the corresponding BF image is photographed under the operating reflection $\mathbf{g}$ with a deviation parameter w. In each case of obtaining the DF image under the reflection $\mathbf{g}$ with the deviation parameter w, another experiment has been performed in this work by using the reflection $-\mathbf{g}$ with the deviation parameter $-w$ for the BF image.

In this work we have observed the features of the two-beam dynamical BF and DF images of a small dislocation loop in an annealed $Al_{76}Si_4Mn_{20}$ specimen under five beam directions $\mathbf{B}$, i.e., $\mathbf{B}$ is parallel to the zone axes A, B, C, D, and E successively, by using different operating reflections $\mathbf{g}$, and with different deviation parameters w.

The main results and corresponding simulations are reported as follows and summarized in Table I.

(1) Zone axis A ($\mathbf{B}\parallel[100001]$).—Figures 2(a) and 2(b) show two-beam dynamical BF and DF images, respectively, with typical black-white lobe contrast, of an annealed $Al_{76}Si_4Mn_{20}$ specimen. The operating reflections are $\mathbf{g}_B=(1\bar{1}121\bar{1})$ for the BF image and $-\mathbf{g}_B=-(1\bar{1}121\bar{1})$ for the DF image. Figures 2(c) and 2(d) are corresponding computer-simulated images with the following parameters: $\mathbf{B}\parallel[100001]$, $\mathbf{b}\parallel\mathbf{n}\parallel[100100]$, $\mathbf{F}\parallel[310002]$, $t=4.5\xi_g$, $d=(4.5-0.188)\xi_g$, where $\mathbf{b}$ is the Burgers vector and $\mathbf{n}$ the normal of the dislocation loop, $\mathbf{F}$ designates the foil normal, $\mathbf{B}$ the electron beam direction, t the foil thickness, and d the depth of the center of the loop measured along the $\mathbf{F}$ direction. For the simulation of the BF image [Fig. 2(c)] $\mathbf{g}_B=(1\bar{1}121\bar{1})$ and $w=-1.5$ have been used. For the DF image [Fig. 2(d)] $-\mathbf{g}_B=-(1\bar{1}121\bar{1})$ and $w=1.5$ have been used. When the operating reflection $\mathbf{g}$ is changed to $\mathbf{g}_A=(11\bar{2}1\bar{1}\bar{1})$, no contrast can be observed. The contrast becomes irregular when $\mathbf{g}$ is parallel to any twofold axis belonging to the zone axis A.

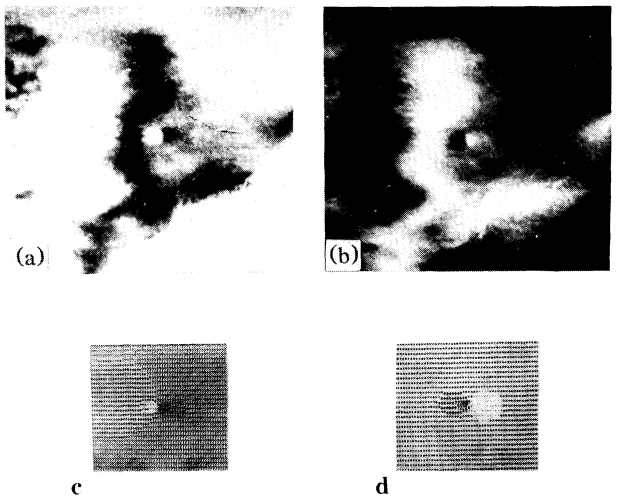

FIG. 2. Black-white contrast images of a small dislocation loop in annealed $Al_{76}Si_4Mn_{20}$ i phase. (a),(b) Experimental images with $\mathbf{B}\parallel[100001]$. (c),(d) Computer-simulated images with the following parameters: $\mathbf{b}\parallel\mathbf{n}\parallel[100100]$, $\mathbf{F}\parallel[310002]$, $t=4.5\xi_g$, $d=(4.5-0.188)\xi_g$. (a),(c) BF, $\mathbf{g}=(1\bar{1}121\bar{1})$, $w=-1.5$. (b),(d) DF, $\mathbf{g}=-(1\bar{1}121\bar{1})$, $w=1.5$.

The upper part of Fig. 3 shows the BF contrast variation with the deviation parameter w when $\mathbf{g}_B=(1\bar{1}121\bar{1})$ is used as the operating reflection. With w increased from a negative value, corresponding to symmetrical incidence ($w=-3.4$), to a positive value, the contrast of the BF image changes according to the following sequence, black dot → white-black lobe → white dot → black-white lobe → black dot, when viewed along the $\mathbf{g}$ direction. It means a reversal of the black-white lobe with w. The contrast of the DF image is nearly complementary to that of the corresponding BF image. By using $-\mathbf{g}_B=-(1\bar{1}121\bar{1})$ as the operating reflection, the same phenomenon has been observed when viewed along the direction of the operating reflection $\mathbf{g}$ ($\mathbf{g}=-\mathbf{g}_B$).

The lower part of Fig. 3 is a series of computer-simulated BF images with the following parameters: $\mathbf{B}\parallel[100001]$, $\mathbf{g}=(1\bar{1}121\bar{1})$, $\mathbf{b}\parallel\mathbf{n}\parallel[100100]$, $\mathbf{F}\parallel[310002]$, $t=4.5\xi_g$, $d=(4.5-0.188)\xi_g$, and $w=-4.0$, -1.5, 0.0, 1.25, and 3.5, respectively, from the left-hand side to the right-hand side of the figure, corresponding to the experimental images shown in the upper part of Fig. 3.

(2) Zone axis B ($\mathbf{B}\parallel[100010]$).—No contrast has been observed under the operating reflections $\mathbf{g}_A=(11\bar{2}1\bar{1}\bar{1})$ and $\mathbf{g}_C=(121\bar{1}\bar{1}1)$.

(3) Zone axis C ($\mathbf{B}\parallel[000011]$).—Irregular contrast has been observed under $\mathbf{g}_B=(1\bar{1}121\bar{1})$ but no contrast

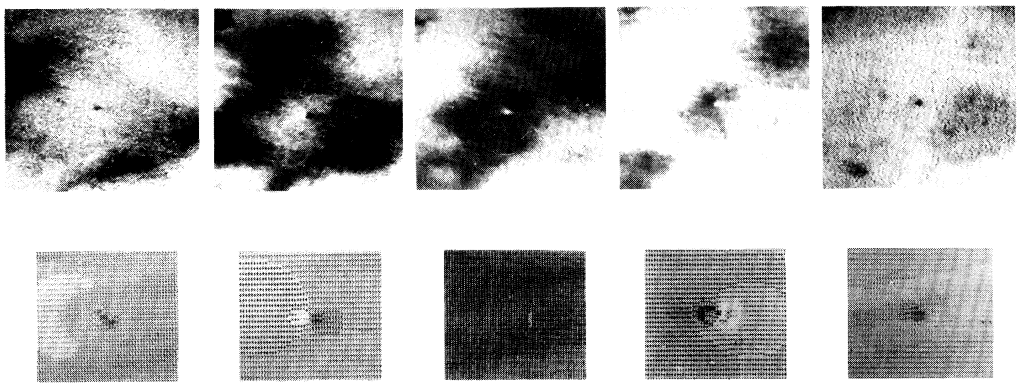

FIG. 3. BF contrast variation of the small dislocation loop in annealed $Al_{76}Si_4Mn_{20}$ *i* phase with deviation parameter *w*. $\mathbf{B}\|[100001]$, $\mathbf{g}=(1\bar{1}121\bar{1})$. Upper part: The experimental BF images with *w* increasing from a negative value to a positive value. Lower part: The computer-simulated images with the parameters $\mathbf{B}\|[100001]$; $\mathbf{g}=(1\bar{1}121\bar{1})$; $\mathbf{b}\|\mathbf{n}\|[100100]$; $\mathbf{F}\|[310002]$; $t=4.5\xi_g$; $d=(4.5-0.188)\xi_g$; $w=-4.0$, -1.5, 0.0, 1.25, and 3.5, respectively, from the left-hand side to the right-hand side.

under $\mathbf{g}_C=(121\bar{1}\bar{1}1)$.

(4) Zone axis D ($\mathbf{B}\|[110000]$).—By using $\mathbf{g}_B=(1\bar{1}121\bar{1})$ or $-\mathbf{g}_B$ as the operating reflection, the BF contrast changes, with *w* increased from negative to positive values, according to the following sequence: black dot → black-white lobe → white dot → white-black lobe → black dot, when viewed along the direction of the operating reflection. The DF images show nearly complementary contrast to that of the corresponding BF images. Compared with the case of $\mathbf{B}\|[100001]$ (zone axis *A*), the contrast-reversal behavior is just the opposite, although the same operating reflection $\mathbf{g}_B$ is used. Under the operating reflection $\pm\mathbf{g}_D=\pm(1\bar{1}\bar{1}121)$ only weak irregular contrasts have been observed.

(5) Zone axis E ($\mathbf{B}\|[010001]$).—Irregular contrast has been observed under $\pm\mathbf{g}_D=\pm(1\bar{1}\bar{1}121)$ but no contrast under $\pm\mathbf{g}_A=\pm(1121\bar{1}\bar{1})$.

By summarizing the above-mentioned observations it is obvious that there is no contrast under the operating reflections $\pm\mathbf{g}_A$ and $\pm\mathbf{g}_C$. The contrast is irregular when $\pm\mathbf{g}_D$ is used. Black-white lobe contrast may be observed only when $\pm\mathbf{g}_B=\pm(1\bar{1}121\bar{1})$ is chosen as the operating reflection. All of these phenomena have been simulated successfully by using the parameters listed in section (1), except the beam direction **B**, operating reflection **g**, and deviation parameter *w*, which are different for different experimental conditions.

According to Wang and Cheng,[13] the dynamical theory of electron diffraction for crystals can be extended to the case of quasicrystals if the term $\mathbf{g}\cdot\mathbf{R}$ is replaced by the inner product $\tilde{\mathbf{g}}\cdot\tilde{\mathbf{R}}=\mathbf{g}\cdot\mathbf{R}+\mathbf{g}^{\perp}\cdot\mathbf{R}^{\perp}$ in higher-dimensional space, where the term $\mathbf{g}^{\perp}\cdot\mathbf{R}^{\perp}$ represents the effect caused by the phason. Therefore, many conclusions about the diffraction contrast in the case of crystals can also be extended to the case of quasicrystals.

As summarized by Edington,[4] in the case of crystals, besides small dislocation loops, other small defects, such as end-on dislocation lines, gas bubbles, voids, and small precipitates, may also show black-white lobe contrast. An end-on dislocation line may appear as a line contrast when the foil is tilted by a large angle. In the present work we have observed the diffraction contrast of the defect under five zone axes. The angles between these axes are 36°, 60°, and 72°, but we have never observed any line contrast. This fact excludes the possibility of the end-on dislocation. The contrast image of a gas bubble or a void will appear as a bright dot when it is underfocused under the kinematical condition, and as a dark dot when overfocused. By this means these possibilities may easily be excluded. A small spherical (or nearly spherical) precipitate appears as a black-white lobe under the two-beam dynamical condition with its ***l*** vector, pointed from the center of the black lobe to the center of the white lobe, parallel (or nearly parallel) to the operating reflection **g**. Our observations show that the contrast image is changed from black-white lobe for $\mathbf{g}_B=(1\bar{1}121\bar{1})$ to irregular contrast for $\mathbf{g}_D=(1\bar{1}\bar{1}121)$, and even to no contrast for $\mathbf{g}_A=(1121\bar{1}\bar{1})$ and $\mathbf{g}_C=(121\bar{1}\bar{1}1)$. This fact excludes the possibility of a small spherical or nearly spherical inclusion. Moreover, the agreement between the experimental and simulated images, by taking the same series of parameters as listed in section (1) and taking corresponding beam directions **B**, operating reflections **g**, and deviation parameters *w*, strongly supports the conclusion that the defect we have observed is a small dislocation loop.

The variation of the contrast features with the deviation parameter *w* for *i* phase as observed in this work, i.e., the reversal of the black-white lobe, is quite different compared with that for crystals. The success of the computer simulation of this phenomenon shows that this peculiar phenomenon may be caused by the phason strain field of the small dislocation loop in *i* phase.

There also exists a depth oscillation of the contrast of

a small dislocation loop in i phase as in the case of crystals.[1] The effective depth z_0 of the loop, measured along the beam direction **B**, is different for different beam directions. This may explain the different contrast features when using the same operating reflection $\mathbf{g}_B$ but different beam directions, as described in sections (1), (3), and (4).

We have chosen the Burgers vector **b** of the small dislocation loop to be parallel to the twofold symmetry axis [100100], which is in agreement with the identification reported by Zhang, Wollgarten, and Urban[9] for the dislocation lines in $Al_{65}Cu_{20}Fe_{15}$ i phase. But we are not sure whether the dislocation loop is of the interstitial type ($\mathbf{b}\parallel -\mathbf{n}$) or the vacancy type ($\mathbf{b}\parallel\mathbf{n}$) because the contrast shows a depth-oscillation behavior and we have not measured experimentally the true depth of the loop center.

This project is supported by the National Natural Science Foundation of the People's Republic of China.

[1]M. Wilkens, in *Diffraction and Imaging Techniques in Materials Science,* edited by S. Amelinckx, R. Gevers, and J. Van Landuyt (North-Holland, Amsterdam, 1978), p. 185.

[2]D. K. Saldin, A.Y. Stathopoulos, and M. J. Whelan, in *Electron Diffraction 1927–1977,* edited by P. J. Dobson, J. B. Pendry, and C. J. Humphreys, Inst. Phys. Conf. Ser. No. 41 (The Institute of Physics, London, Bristol, 1978), p. 350.

[3]C. A. English, B. L. Eyre, S. M. Holmes, and R. C. Perrin, in *Electron Diffraction 1927–1977* (Ref. 2).

[4]J. W. Edington, *Practical Electron Microscopy in Materials Science* (MacMillan, London, 1975), Vol. 1, p. 11; Vol. 3, p. 32; and Vol. 4, p. 6.

[5]D. Shechtman, I. Blech, D. Gratias, and J. W. Cahn, Phys. Rev. Lett. **53**, 1951 (1984).

[6]D. Levine, T. C. Lubensky, S. Ostlund, S. Ramaswamy, P. J. Steinhardt, and J. Toner, Phys. Rev. Lett. **54**, 1520 (1985).

[7]J. E. S. Socolar, T. C. Lubensky, and P. J. Steinhardt, Phys. Rev. B **34**, 3345 (1986).

[8]M. Hirabayashi and K. Hiraga, Mater. Sci. Forum **22-24**, 45 (1987).

[9]Z. Zhang, M. Wollgarten, and K. Urban, Philos. Mag. Lett. **61**, 125 (1990).

[10]M. Dai and R. Wang, Solid State Commun. **73**, 77 (1990).

[11]R. Wang and M. Dai, Philos. Mag. Lett. **61**, 119 (1990).

[12]Y. Cheng and R. Wang, Solid State Commun. **68**, 795 (1988).

[13]R. Wang and Y. Cheng, Mater. Sci. Forum **22-24**, 409 (1987).

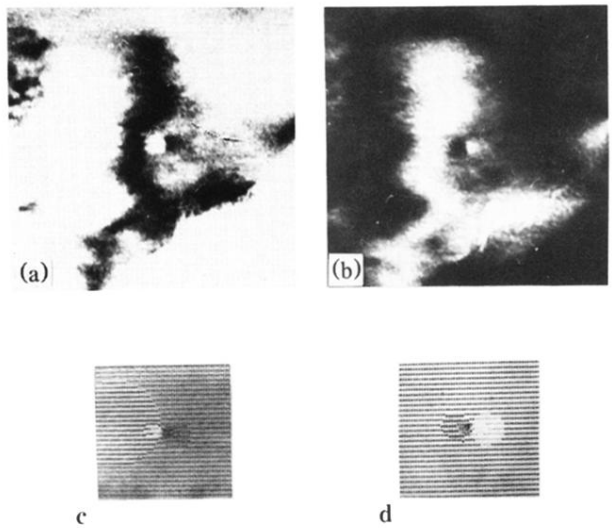

FIG. 2. Black-white contrast images of a small dislocation loop in annealed $Al_{76}Si_4Mn_{20}$ *i* phase. (a),(b) Experimental images with $\mathbf{B}\parallel[100001]$. (c),(d) Computer-simulated images with the following parameters: $\mathbf{b}\parallel\mathbf{n}\parallel[100100]$, $\mathbf{F}\parallel[310002]$, $t=4.5\xi_g$, $d=(4.5-0.188)\xi_g$. (a),(c) BF, $\mathbf{g}=(1\bar{1}121\bar{1})$, $w=-1.5$. (b),(d) DF, $\mathbf{g}=-(1\bar{1}121\bar{1})$, $w=1.5$.

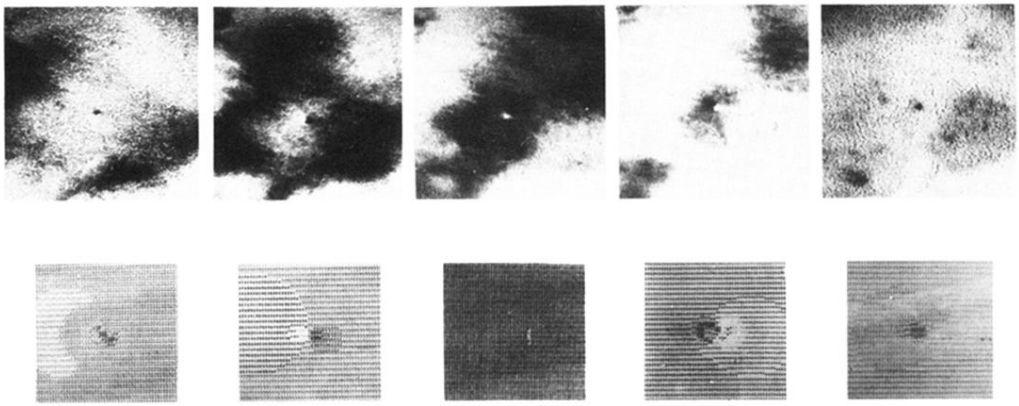

FIG. 3. BF contrast variation of the small dislocation loop in annealed $Al_{76}Si_4Mn_{20}$ i phase with deviation parameter w. $\mathbf{B}\|[100001]$, $\mathbf{g}=(1\bar{1}121\bar{1})$. Upper part: The experimental BF images with w increasing from a negative value to a positive value. Lower part: The computer-simulated images with the parameters $\mathbf{B}\|[100001]$; $\mathbf{g}=(1\bar{1}121\bar{1})$; $\mathbf{b}\|\mathbf{n}\|[100100]$; $\mathbf{F}\|[310002]$; $t=4.5\xi_g$; $d=(4.5-0.188)\xi_g$; $w=-4.0$, -1.5, 0.0, 1.25, and 3.5, respectively, from the left-hand side to the right-hand side.